Strain relaxation in different shapes of single crystal graphene grown by chemical vapor deposition on copper

Tharanga R. Nanayakkara, U. Kushan Wijewardena, Sajith M. Withanage, Annika Kriisa, Rasanga L. Samaraweera, Ramesh G. Mani

PII: S0008-6223(20)30686-2

DOI: https://doi.org/10.1016/j.carbon.2020.07.025

Reference: **CARBON 15495** 

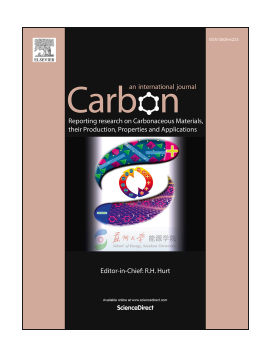
To appear in: Carbon

Received Date: 7 May 2020 Revised Date: 7 July 2020 Accepted Date: 11 July 2020

Please cite this article as: T.R. Nanayakkara, U.K. Wijewardena, S.M. Withanage, A. Kriisa, R.L. Samaraweera, R.G. Mani, Strain relaxation in different shapes of single crystal graphene grown by chemical vapor deposition on copper, Carbon (2020), doi: https://doi.org/10.1016/j.carbon.2020.07.025.

This is a PDF file of an article that has undergone enhancements after acceptance, such as the addition of a cover page and metadata, and formatting for readability, but it is not yet the definitive version of record. This version will undergo additional copyediting, typesetting and review before it is published in its final form, but we are providing this version to give early visibility of the article. Please note that, during the production process, errors may be discovered which could affect the content, and all legal disclaimers that apply to the journal pertain.

© 2020 Published by Elsevier Ltd.



Tharanga R. Nanayakkara Conceptualization, Methodology, Validation, Formal analysis,

Software, Writing - Original Draft

U. Kushan Wijewardena Formal analysis, Software, Visualization

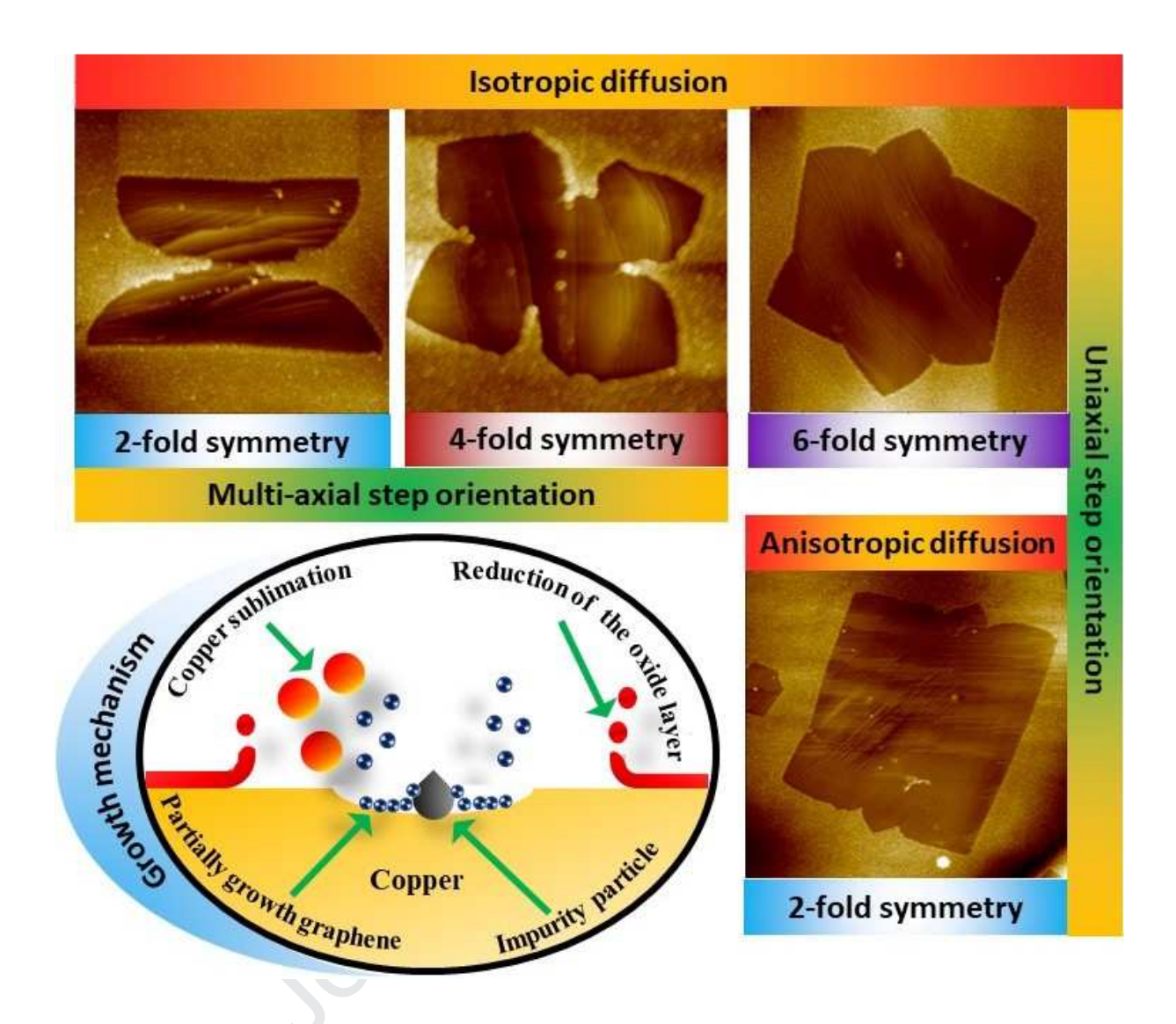
Sajith M. Withanage Methodology, Validation, Software

Annika Kriisa Methodology, Formal analysis

Rasanga L. Samaraweera Methodology, Validation

Ramesh G. Mani Conceptualization, Investigation, Supervision, Writing - Review

& Editing



# Strain Relaxation in Different Shapes of Single Crystal Graphene Grown by Chemical Vapor Deposition on Copper

Tharanga R. Nanayakkara\*<sup>2</sup>, U. Kushan Wijewardena, Sajith M. Withanage, Annika Kriisa, Rasanga L. Samaraweera†, Ramesh G. Mani\*<sup>1</sup>

Department of Physics and Astronomy, Georgia State University, Atlanta, Georgia 30303, USA

#### **Abstract**

The chemical vapor deposition (CVD) growth of single-crystal graphene on polycrystalline copper foils is a complex process affected by thermodynamics, kinetics, and growth conditions. These factors lead to the diversity of island shapes of single crystal graphene. Here, we present an experimental atomic force microscopy (AFM) study of the different shapes of single-crystal graphene grown on the inner surface of copper enclosures using the low pressure CVD technique. Most remarkably, this study indicates that graphene single crystal appears to form below the adjacent copper foil surface. This feature is revealed in cross sectional AFM scans of the height, which indicate that the graphene surface lies below the neighboring foil surface by ~15- 30 nm. Our results also show that an impurity assisted growth mechanism governs the growth of single crystal graphene via isotropic diffusion, producing two-fold, four-fold, and six-fold symmetries in the resulting flakes. In addition, single crystal graphene produced via anisotropic diffusion is also present here, but they do not exhibit signs of an impurity assisted growth mechanism. Finally, we find that strain relaxation in two-fold and four-fold symmetric graphene structures via isotropic diffusion are more complicated than the six-fold structures via isotropic diffusion, which results in multiple steps orientations in low symmetry structures.

<sup>\*</sup> Corresponding author. Tel.: +1-404-413-6060.

#### 1. Introduction

Graphene [1], which is a single two-dimensional layer of carbon atoms organized in a hexagonal structure, has attracted great interest due to its intriguing electronic properties [2, 3] and its promise of living up to expectations as a material of choice for critical future electronics applications [4-11]. Several methods of graphene growth have been employed, including exfoliation from graphite [12, 13], epitaxial growth on SiC [14, 15], mechanical cleavage from bulk graphite [16], chemical vapor deposition (CVD) [17-22] and the reduction of graphite oxide [23, 24]. Among these methods, the CVD technique has attracted considerable interest since it is a promising method for producing comparatively large-scale, high-quality graphene at a relatively low cost.

The CVD technique utilizing thin transition metal foils of copper [17, 18], nickel [25-28], ruthenium [29, 30], platinum [31], and cobalt [32] have been studied extensively. In these methods, thin foils assist in the decomposition of the carbon groups from the precursor, and also in the nucleation of the graphene crystal. Graphene synthesis on these metal catalysts is affected by factors such as the limit of the carbon solubility in the metal, crystallographic orientation of the metal foil surface, and thermodynamic variables such as growth temperature and pressure [33]. The CVD growth of graphene on copper is attractive since copper is a very low carbon solubility catalyst, graphene growth is restricted to the surface of the catalyst [34-37], and graphene growth is self-limiting, producing a monolayer of graphene since carbon precursor decomposition generally does not occur on top of the deposited graphene [38-40]. Yet, the growth of few-layer graphene on copper has also been reported when the self-limit is broken [41-44] sometimes by specific conditions, such as higher methane concentration [33, 42] and impurity enhanced growth [45]. Graphene growth in CVD starts with the formation of stable nuclei, these nuclei grow and coalesce at the grain boundaries, resulting in the polycrystalline graphene over 100 micron length scales. The polycrystalline morphology degrades the mechanical and electrical properties of graphene, which is undesirable for graphene applications. Thus the development of growth techniques to reduce the density of two-dimensional grain boundaries is a topic of interest in graphene growth.

In an attempt to control these issues, work has been carried out using techniques such as electro polishing of the substrate [20, 40, 46-49], the two step CVD process [50], seeded growth

CVD technique [51, 52], oxygen assisted CVD [53], plasma assisted CVD technique [54-56], graphene growth on liquid copper [57], and proton assisted CVD growth method [58]. Previous works have reported a clear correlation between the shape of the graphene nuclei and the crystal orientation of the underlying copper substrate[38, 59, 60]. In addition, the shape and the size of the graphene nuclei are also influenced by the growth parameters such as pressure [44, 59, 61-63], temperature [50, 63], cooling rates [64], precursors composition and flux [43, 65]. These factors have been investigated both experimentally and theoretically. The theoretical study of the morphological evolution during the crystal growth are mostly based on the phase field theory [53, 60, 66, 67], and Monte Carlo simulations [68, 69]. Yet, the mechanisms that govern the shape dynamics of graphene nuclei in the CVD growth are still not fully understood.

In addition, the corrugations appearing on the copper surface in conjunction with graphene growth degrades the quality of graphene since those corrugations lead to surface defects and wrinkles which significantly affect the properties of the graphene. The terraced steps/ripples on the copper surface during the CVD could be due to pining of the moving copper atoms below the graphene surface [70, 71], stress relaxation between copper and graphene [72] and dynamic phase instability of carbon and copper [73]. During the cooling stage in the CVD process, there is thermal stress at the copper and graphene interface due to mismatch of thermal expansion coefficients of graphene(-7×10<sup>-6</sup> K<sup>-1</sup>) [74] and copper(18×10<sup>-6</sup> K<sup>-1</sup>). The mismatch and opposite signs in the thermal expansion coefficients results in an expansion of graphene and a contraction of copper with a decrease of the temperature. As a consequence of this, the copper surface gets rough and the graphene forms wrinkles [75]. The role of these factors in the topography of graphene flakes could also be better understood.

In this work, we utilized low pressure CVD (LPCVD) technique to produce graphene single crystals. We used atomic force microscope (AFM) to examine the growth morphologies of the graphene flakes in copper domains with different crystal orientations. A common feature observed in this study is that the graphene flakes lie ~15-30 nm below the adjacent surface. Our results also show that impurity assisted growth results in isotropic growth of single crystal graphene with two-fold, four-fold, and six-fold symmetries. At the same time, however, anisotropic graphene single crystals, also observed in this study, did not exhibit signs of impurity assisted growth. We also examine the strain relaxation in single crystals of different symmetry

and suggest that the multiple step orientations observed in lower symmetry structures reflect the strain relaxation process, which is not as in higher symmetry structures.

# 2. Experimental section

# 2.1 Synthesis of Graphene

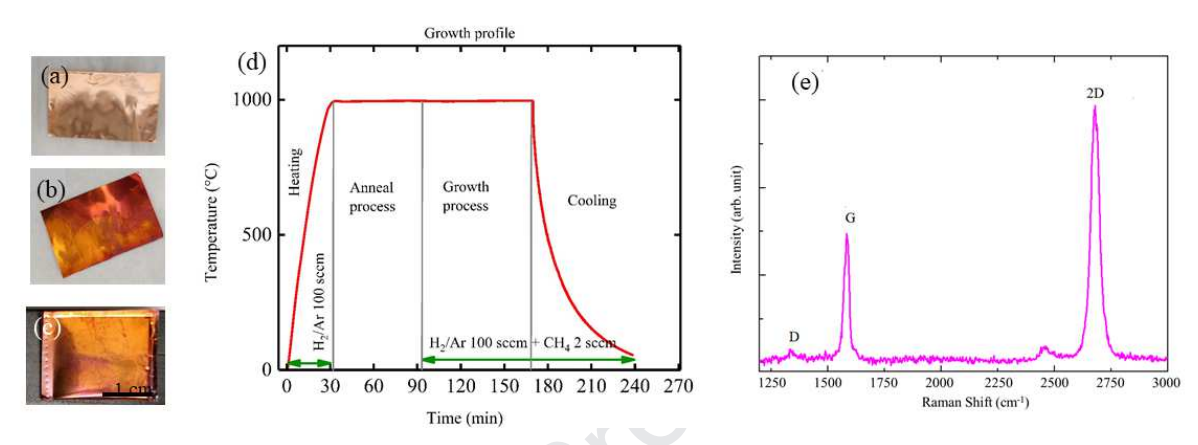


Fig. 1. Preparation of copper foils and the growth of graphene. (a) This panel shows the copper foil after the rinse of the foil with acetone, methanol and deionized water. (b) Dried copper foil pre-oxidized for 15 min on a hot plate under ambient conditions turned to a reddish color as shown in here. (c) The oxidized copper foil is folded into an enclosure. This copper enclosure was placed within a home built CVD system for graphene growth. (d) This panel describes the graphene growth profile utilized in this work. Note that copper enclosure was annealed without  $H_2/Ar$  flow. (e) Raman measurements on of CVD graphene on  $Si/SiO_2$  indicate monolayers.

Commercially available 25  $\mu$ m thick copper foil was utilized in this CVD growth study. The foils were initially rinsed with acetone, methanol, and deionized water respectively. Both sides of the dried copper foil were then pre-oxidized [19, 76, 77] on a hot plate for 15 minutes under ambient conditions and then, a copper enclosure was made for the LPCVD as shown in Fig. 1(c). The copper enclosure was loaded into a 1-inch quartz tube mounted inside a tube furnace. The CVD system was pumped down from ambient pressure to ~40 mTorr. Next,  $H_2/Ar$  gas mixture was introduced into the CVD chamber and the chamber pressure rose to ~340 mTorr. Subsequently, the copper enclosure was heated up to ~1000 °C. Upon reaching 1000 °C, the  $H_2/Ar$  flow was shut off and the copper enclosure was then annealed in that state for ~60 minutes. Then, the  $H_2/Ar$  and  $CH_4$  gaseous species were introduced to the CVD chamber simultaneously, with desired flow rates for growth of graphene as shown in Fig. 1(d). After growth, the system was cooled to room temperature by shutting off the heating coils and simply opening the furnace. A post-growth thermal anneal in an oven, for 5 min at 150 °C, served to help visualize graphene grown on the copper surface [78].

#### 2.2 Characterization

A Park XE7 AFM served to examine the diverse growth morphologies of the graphene. AFM images were obtained under ambient conditions, roughly two days after the growth as the samples were stored under ambient conditions during this time. We calculated the root mean squared smoothness by analyzing AFM topographical images to compare the surface smoothness of the grown graphene relative to the neighboring copper surface where there was no graphene. We introduce the parameters  $\lambda$ , which is the average distance between two adjacent steps, and  $\Delta S_q$  which represents the relative root mean squared smoothness, expressed as a percentage, in reporting the results (see supplementary information for more detail).

#### 3. Results and discussion

In this study, we applied a pre-anneal process to the copper surface under ambient conditions to suppress the nucleation density of graphene on oxygen rich copper surface, as described in previous studies [44, 52, 76]. We used a copper enclosure to realize these results, and all the shapes described here are observed on the inner surface of the copper enclosure. We note that comparatively small-sized graphene domains with a very high nucleation density appeared in the outer surface of the copper enclosure. The optical microscope images on inner surface of enclosure suggest a variation in the density of graphene structures along the direction of gas flow within the CVD system with greater density upstream in comparison to the downstream areas (see supplementary information Fig. S2).

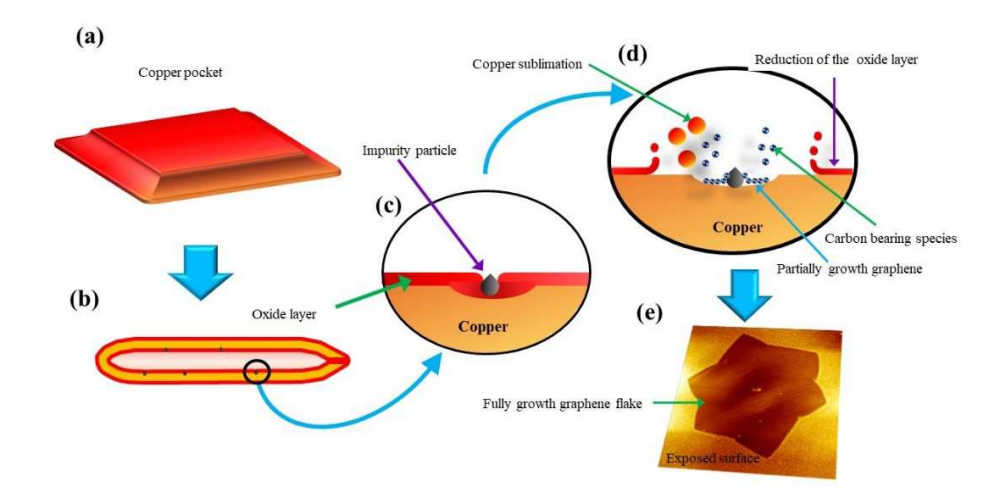


Fig. 2. Schematic diagram illustrates the possible growth mechanism of single crystal graphene on the inner surface of the copper enclosure used in this study (not in scale). (a) The oxidized copper foil is folded into a pocket. (b) Cross view of the copper pocket. The red outline represents the oxide layer in both the inner and outer surfaces of the pocket. Yellow intermediate layer depicts the non-oxidized copper region while black dots show the impurity particles (c) This panel shows the magnified area which is circled in panel (b). (d) The oxide layer is released from the surface more effectively around the impurity particle by promoting the copper sublimation at low pressure. Nucleation could start on impurity particle. (e) Top view of a single crystal graphene flake, which is appears to lie below the adjacent exposed surface.

Fig. 2 depicts a possible impurity assisted growth mechanism of the single crystal graphene. Here, the nucleation could be initiated by an impurity particle on the copper surface. These impurity particles could have been introduced on to the copper surface during the oxidation under ambient conditions. The possibility of impurities acting as seeds for nucleation has been considered before [52]. However, the impurity appears to be larger in our case. The oxide layer is released from the surface more effectively around the impurity particle by promoting the copper sublimation at low pressure [79] during the anneal and growth process. The gas precursors could enter the inside of the copper enclosure through gaps at the edge of the enclosure and possibly by diffusion through the walls of the enclosure. Then, the nucleation could start on the impurity nanoparticle [52] and continues the growth of graphene on fresh copper, below the adjacent surface as shown Fig. 2(d). Hence, it appears that the graphene grows below the adjacent exposed surface. Our AFM topographic study indicates that all the single crystal graphene flakes observed here are sunk 15~30 nm below the adjacent surface. Further we confirmed that observable flake patterns are composed by graphene and there is no graphene outside the observable patterns (see supplementary information for more detail).

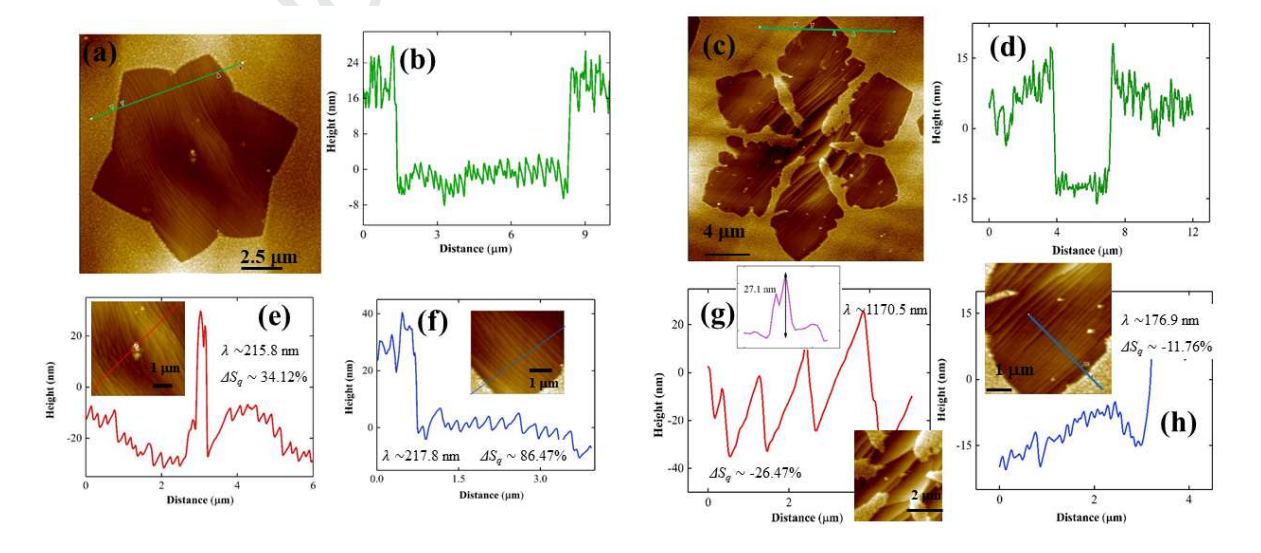


Fig. 3. The atomic force microscope topographical map of graphene flakes on the copper surface exhibiting six-fold symmetry. The areas of the dark contrast are graphene and the bright areas are the exposed regions where no graphene. (a) The star like polygon shape of graphene flake with six lobes with isotropic diffusion along the vertices. This graphene flake appears to be ~24 nm below the exposed copper foil surface as shown in panel (b) which is the height profile along the green line in panel (a). (e) and (f) describe the height profiles on the nanosteps appearing in (a) on the center and dendritic regions of the flake, respectively. (c) This panel depicts the microscale flower shape of graphene with six-fold symmetry. Growth of this flake suggests isotropic diffusion along the vertices as a ~27 nm impurity nanoparticle appears at the geometric center of the graphene flake as shown in insert of panel (g). Panel (d) shows the height profile along the green line in (c) which suggests that the graphene flake in (c) lies below the exposed copper surface. (g) represents the height profile of nanosteps at center of the crystal in (c) while (h) shows the height profile in wide dendritic region. Here,  $\lambda$  is the average distance between two adjacent steps and  $\Delta S_q$  is the relative root mean squared smoothness of the graphene surface, expressed as a percentage.

Fig. 3 shows topographic AFM images of single crystal graphene with six-fold growth symmetry on copper. The dark areas are graphene and the bright areas are the adjacent foils areas. Fig. 3(a) exhibits a star-like graphene flake with six lobes. Generally, the six-fold symmetry of this type of flake follows the underlying crystal orientation of the copper surface, i.e., the six-fold symmetry mostly reflects the Cu(111) facet [38, 60, 68]. In these structures, the graphene growth rate along the six vertices are approximately the same due to isotropic diffusion of carbon species. Considering its six-fold symmetry, the nucleation starting point would be the geometric center of the flake. A close scrutiny reveals the existence of a single nanoparticle at the geometric center of the graphene island as shown height profile in Fig. 3(e). The nanoparticle served as the nucleation center for graphene growth and suggests an impurity assisted growth mechanism. Note also that periodic nano-scaled steps appear in the graphene flakes due to possible strain relaxation during the CVD cooling process due to different thermal expansion coefficient of copper and graphene. The measured distance between steps,  $\lambda$ , at different locations on this graphene flake are approximately the same and this feature suggests a single layer of the graphene since the  $\lambda$  is expected to change with number of layers [80]. Also, according to the  $\Delta S_q$  values, the surface of this flake is smoother than the adjacent exposed surface without graphene.

A graphene flake with a flower-like shape and six-fold symmetry, and the fractal-like features in the lobes area, is presented in Fig. 3(c). This shape could arise if there is possible graphene etching during the growth process. Graphene growth and etching processes are inversely related to each other [81] that should approach a dynamic equilibrium during the CVD in order to result in the regular flake shapes with sharp edges. It is known that hydrogen plays a dual role in the CVD growth process. As an activator, it leads to growth, and as an etchant, it acts to manipulate the size and the morphology of graphene island [82, 83]. The narrowed copper step-bunching

appeared at the lobes areas while broadened copper step-bunching appeared at the center area as shown in Fig. 3(h) and (g), respectively. The graphene flake in Fig. 3(c) appears rougher than the adjacent exposed regions since it has large sized terrace steps.

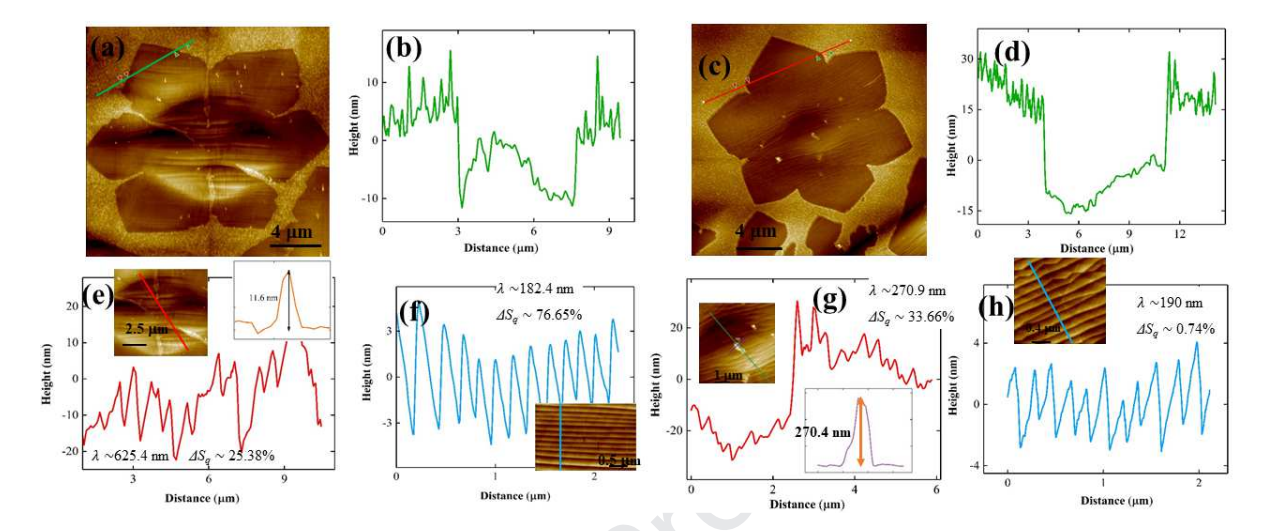


Fig. 4. The AFM topographical images of CVD growth graphene crystals on the copper surface. The areas of the dark contrast are graphene and the bright areas are regions without graphene. (a) exhibits the microscale graphene 'flower' with the six-fold symmetry and isotropic diffusion along the vertices as a 11.6 nm height impurity nanoparticle appears at the center of the graphene island as shown in panel (e) insert. Panel (b) shows the height profile along the green line in (a), and it indicates that the graphene flake lies below the copper surface. (e) and (f) show the height profiles of the terraced steps formed at the center and lobe of graphene flake in (a), respectively. Panel (c) shows the flower shaped graphene flake with an isotropic diffusion pattern. A nanoparticle with a height of ~270 nm appeared at the geometric center of the flake as shown in lower inset of panel (g). (d) depicts the height profile along the red line in (c) which confirms that the graphene flake lies below the adjacent surface. (g) and (h) represent the height profiles of the terraced steps formed at the center and lobe of graphene flake in (c), respectively. Here,  $\lambda$  is the average distance between two adjacent steps and  $\Delta S_q$  is the relative root mean squared smoothness of the graphene surface, expressed as a percentage.

Fig. 4(a) shows a nearly hexagonal graphene crystal with six-fold symmetry. This flake appears ~15 nm below the surface as indicated by the height profile in Fig. 4(b). Possibly, the growth process started at the geometric center, which also shows a wavy nature at the surface close to the center of the flake. The observed protuberance near the center is attributed to the different thermal expansion coefficients of graphene and copper. The lobes in this flake show a wide dendritic contour except for the one lobe which is the closest one to a neighboring graphene crystal. This may suggest a possible growth competition—among the flakes due to low concentration of localized active carbon species around them. Concentration of precursor is one of the crucial factors in determining the morphology of graphene flakes [66]. Another peculiar topographic feature is the wavy nature with a convex shape at the center of the graphene flakes,

as shown in Fig. 4(c). This convex nature looks different in comparison to previously reported graphene, which exhibited vermicular features due to interfacial stability [73]. Here, the steps protected their orientations even on the convex region. This convex feature exhibits a wavy nature as clearly seen in Fig. 4(g) and nucleation could start at this center. The convex feature is a result of strain relaxation of graphene during the cooling due to different thermal expansion with copper. Also, this wavy nature reflects the weak coupling between graphene and the copper substrate. The measured  $\lambda$  values are different in center area and edge area of graphene flakes suggesting the possibility of nucleation of a second layer near the center of the flake [80].

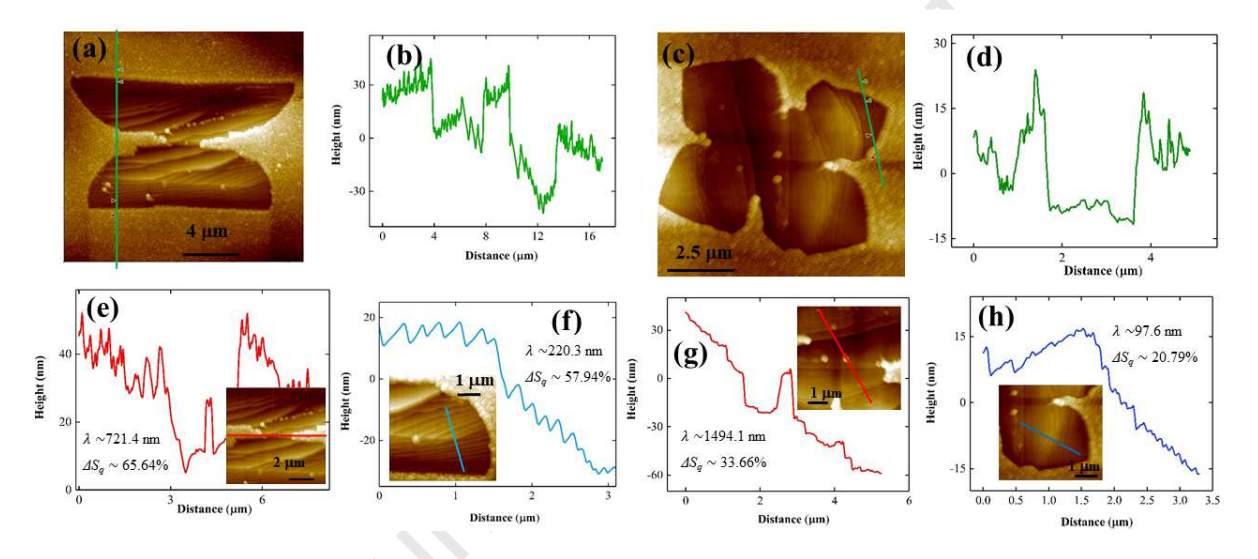


Fig. 5. Atomic force microscope topographical images of graphene flakes with two fold and four fold symmetries on the copper surface. The dark areas are graphene and the bright areas are the exposed regions. Panel (a) exhibits an hour glass shape with two-fold symmetry and an impurity nanoparticle with ~15.9 nm height at the center of the flake. This flake is observed below the adjacent exposed surface as shown in (b) which is the height profile along the green line in (a). Panel (c) shows a flower like crystal of graphene including four petals indicating a four-fold symmetry with isotropic diffusion along the four vertices and an impurity nanoparticle with ~27 nm height at the center of the graphene domain. Panel (d) shows the height profile along the green line in (c), which confirms the existence of graphene flake below the adjacent exposed copper foil surface. Panels (e) and (f) present the height profile of the center and lobe area of the graphene island in (a), respectively. (g) and (h) are the height profile of the center and lobe area of the graphene island in (c), respectively. Here,  $\lambda$  is the average distance between two adjacent ripples/steps and  $\Delta S_q$  is the relative root mean squared smoothness, expressed as a percentage, of the graphene surface.

Fig. 5 presents AFM topographical images of graphene crystals with two-fold and four-fold symmetry. Fig. 5(a) shows clear "hourglass" shapes of single crystal graphene with two-fold symmetry. The terrace steps on this flake are less dense close to neck area and highly dense near the edges of two receptacles of the flake as shown in Fig. 5(e) and 5(f), respectively. An impurity nano particle appeared at the geometric center of this structure as shown in Fig. 5(e). Graphene flakes with this topography are rarely observed in CVD graphene because they form on a high

index facet of copper [60]. Fig. 5(c) exhibits the graphene island with four-fold symmetry. Four-fold symmetric graphene domains have been reported on Cu(100) surface previously [60]. An impurity nanoparticle is present close to the geometric center of this graphene flake, as seen in Fig. 5(g). The steps are denser with narrow crest at the edge of the lobes as shown in Fig. 5(h), while a broader crest appears with less dense steps close to the center of the graphene crystal. Unlike in six-fold symmetric flakes, several steps orientations appeared in graphene surface on two fold and four fold structures. The multiple step orientations in lower symmetry structures reflect the complicated process in strain relaxation, which is not as in higher symmetry structures.

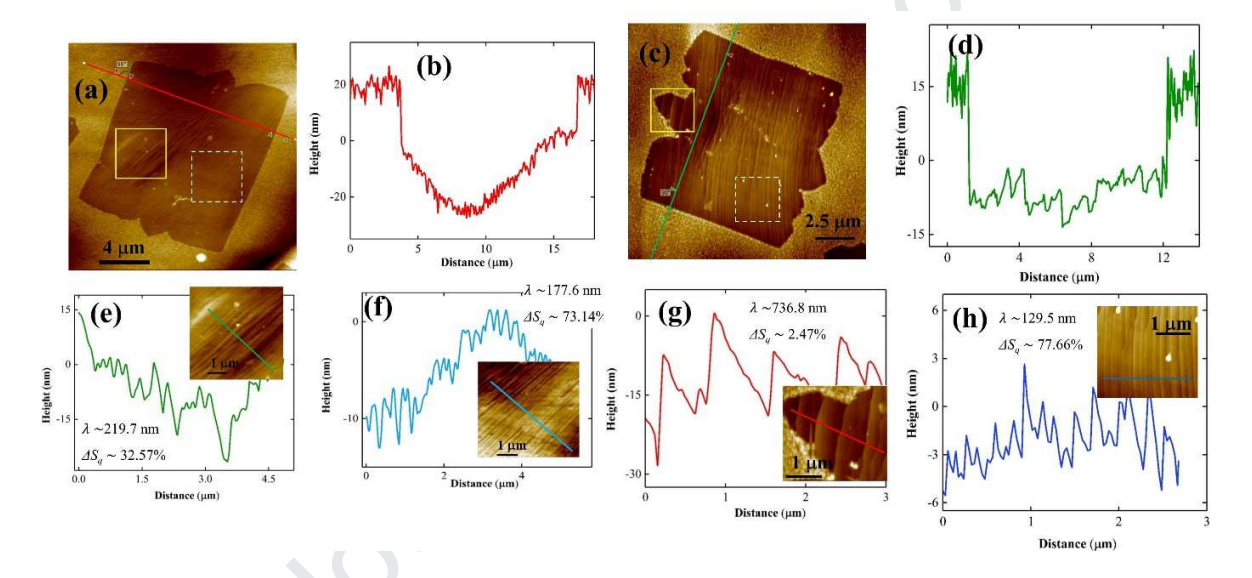


Fig. 6. The characterization of AFM topographical image of the CVD growth graphene flake on copper surface. Panel (a) and (c) show a graphene islands with six-lobes, growth via anisotropic diffusion. These graphene flakes appear to be sunken in to the copper foil surface, as suggested by the height profiles in panel (b) and (d). (e) shows the height profile along the green line in the inset, which lies in the solid yellow square in graphene flake in panel (a). (f) depicts the height profile of nanoscale steps on graphene surface in the area as shown in inset of (f) which is highlighted in dashed white square in panel (a). (g) and (h) show that step edges appear in solid yellow square and dashed white square in graphene flake in panel (c), respectively. Here,  $\lambda$  is the average distance between two adjacent steps and  $\Delta S_q$  relative root mean squared smoothness of the graphene surface, expressed as a percentage.

Fig. 6 depicts six-lobes graphene flakes resulting from a very anisotropic diffusion and they show the two-fold symmetry. The steps show the approximately the same orientation over the entire surface of the graphene flake in each case. In previous study, it was claimed that this type of shapes grows on Cu(310) facet [60]. The impurity assisted growth mechanism may not be valid for these structures, since no signs of impurity particles at the geometric center of graphene nuclei. We suspect that the step driven competitive growth mechanism [84] as a possible growth

mechanism. The wider copper steps bunching appeared at the one edge of the flake while the narrowed copper steps bunching appeared opposite edge of the flakes as shown in Fig. 6(c). We think that step bunching in this graphene domain could be caused by some impurity particle in the copper substrate, which may lead to anomalous step bunching at the one side of the flake.

#### 4. Conclusion

We investigated the growth and strain relaxation in single crystal CVD graphene with different shapes grown on the inner surface of a copper enclosure. The AFM topographical analysis revealed that the single crystal graphene flakes observed here are sunk about 15-30 nm below the adjacent copper surface. Our findings also show that an impurity assisted growth mechanism leads the growth of single crystal graphene via isotropic diffusion, producing two-fold, four-fold, and six-fold symmetries in the resulting flakes. In addition, single crystal graphene produced via anisotropic diffusion behavior is also present here, but they do not exhibit signs of an impurity assisted growth mechanism. However, the steps density and step size are different in each graphene flake, which may be viewed as unique for each flake. Further, our study shows that strain relaxation in two-fold and four-fold symmetry graphene structures via isotropic diffusion are more complicated than the six-fold symmetry structures via isotropic diffusion, which reflects in multiple steps orientations in two-fold and four-fold symmetry structures.

#### **Author information**

†present address of this author is Department of Science and Technology, Uva Wellassa University, Badulla, Sri Lanka, 90000.

### Acknowledgment

The authors gratefully acknowledge support from the funding agencies. This work and all authors were supported by the NSF under Grant No. ECCS-1710302, and by the Army Research Office under Grant No. W911NF-15-1-0433.

#### Notes

The authors declare no competing financial interest.

#### **Abbreviations**

CVD, chemical vapor deposition; LPCVD, low pressure CVD; AFM, atomic force microscope.

#### Reference

- 1. Geim, A.K. and K.S. Novoselov, The rise of graphene. Nature Materials, 2007. 6(3): p. 183-191.
- 2. Castro Neto, A.H., et al., *The electronic properties of graphene*. Reviews of Modern Physics, 2009. **81**(1): p. 109-162.
- 3. Novoselov, K.S., et al., *Two-dimensional gas of massless Dirac fermions in graphene*. Nature, 2005. **438**(7065): p. 197-200.
- 4. Zhang, Y.B., et al., *Direct observation of a widely tunable bandgap in bilayer graphene*. Nature, 2009. **459**(7248): p. 820-823.
- Kim, K., et al., A role for graphene in silicon-based semiconductor devices. Nature, 2011. 479(7373): p. 338-344
- 6. Novoselov, K.S., et al., *A roadmap for graphene*. Nature, 2012. **490**(7419): p. 192-200.
- 7. Mani, R.G., A. Kriisa, and R. Munasinghe, *Radiation-induced magnetoresistance oscillations in monolayer* and bilayer graphene. Scientific Reports, 2019. **9**.
- 8. Xiang, S.H., et al., *Low-temperature quantum transport in CVD-grown single crystal graphene*. Nano Research, 2016. **9**(6): p. 1823-1830.
- 9. Oliaei Motlagh, S.A., et al., *Topological resonance and single-optical-cycle valley polarization in gapped graphene.* Physical Review B, 2019. **100**(11): p. 115431.
- 10. Mani, R.G., et al., Observation of resistively detected hole spin resonance and zero-field pseudo-spin splitting in epitaxial graphene. Nature Communications, 2012. 3 (996):p1-6
- 11. Mani, R.G., Method for determining the residual electron- and hole-densities about the neutrality point over the gate-controlled n ↔ p transition in graphene. Applied Physics Letters, 2016. 108(033507).
- 12. Novoselov, K.S., et al., Electric field effect in atomically thin carbon films. Science, 2004. **306**(5696): p. 666-669.
- 13. Yi, M. and Z.G. Shen, *A review on mechanical exfoliation for the scalable production of graphene*. Journal of Materials Chemistry A, 2015. **3**(22): p. 11700-11715.
- 14. Tison, Y., et al., Grain boundaries in graphene on SiC(0001) substrate. Nano Lett, 2014. 14(11): p. 6382-6.
- 15. de Heer, W.A., et al., *Large area and structured epitaxial graphene produced by confinement controlled sublimation of silicon carbide*. Proceedings of the National Academy of Sciences of the United States of America, 2011. **108**(41): p. 16900-16905.
- 16. Jayasena, B. and S. Subbiah, *A novel mechanical cleavage method for synthesizing few-layer graphenes*. Nanoscale Research Letters, 2011. **6**.
- 17. Li, X.S., et al., Large-Area Synthesis of High-Quality and Uniform Graphene Films on Copper Foils. Science, 2009. **324**(5932): p. 1312-1314.
- 18. Sarajlic, O.I. and R.G. Mani, Mesoscale Scanning Electron and Tunneling Microscopy Study of the Surface Morphology of Thermally Annealed Copper Foils for Graphene Growth. Chemistry of Materials, 2013. 25(9): p. 1643-1648.
- 19. Chen, X., et al., *Chemical vapor deposition growth of 5 mm hexagonal single-crystal graphene from ethanol.* Carbon, 2015. **94**: p. 810-815.
- 20. Wu, X.Y., et al., *Growth of Continuous Monolayer Graphene with Millimeter-sized Domains Using Industrially Safe Conditions*. Scientific Reports, 2016. **6**.
- 21. Bae, S., et al., *Roll-to-roll production of 30-inch graphene films for transparent electrodes.* Nature Nanotechnology, 2010. **5**(8): p. 574-578.
- 22. Wijewardena, U.K., et al., Effects of Long-Time Current Annealing to the Hysteresis in CVD Graphene on SiO2. MRS Advances: p. 1-8.
- 23. Pei, S.F. and H.M. Cheng, The reduction of graphene oxide. Carbon, 2012. 50(9): p. 3210-3228.
- 24. Wijewardena, U.K., S.E. Brown, and X.Q. Wang, *Epoxy-Carbonyl Conformation of Graphene Oxides*. Journal of Physical Chemistry C, 2016. **120**(39): p. 22739-22743.
- 25. Kim, K.S., et al., *Large-scale pattern growth of graphene films for stretchable transparent electrodes.* Nature, 2009. **457**(7230): p. 706-710.
- 26. Reina, A., et al., Large Area, Few-Layer Graphene Films on Arbitrary Substrates by Chemical Vapor Deposition. Nano Letters, 2009. 9(1): p. 30-35.
- 27. Reina, A., et al., *Growth of Large-Area Single- and Bi-Layer Graphene by Controlled Carbon Precipitation on Polycrystalline Ni Surfaces.* Nano Research, 2009. **2**(6): p. 509-516.
- 28. Yu, Q.K., et al., *Graphene segregated on Ni surfaces and transferred to insulators*. Applied Physics Letters, 2008. **93**(11).

- 29. Pan, Y., D.X. Shi, and H.J. Gao, *Formation of graphene on Ru(0001) surface*. Chinese Physics, 2007. **16**(11): p. 3151-3153.
- 30. Sutter, P.W., J.I. Flege, and E.A. Sutter, *Epitaxial graphene on ruthenium*. Nature Materials, 2008. **7**(5): p. 406-411.
- 31. Ma, T., et al., *Edge-controlled growth and kinetics of single-crystal graphene domains by chemical vapor deposition.* Proceedings of the National Academy of Sciences of the United States of America, 2013. **110**(51): p. 20386-20391.
- 32. Vaari, J., J. Lahtinen, and P. Hautojarvi, *The adsorption and decomposition of acetylene on clean and K-covered Co(0001)*. Catalysis Letters, 1997. **44**(1-2): p. 43-49.
- 33. Bhaviripudi, S., et al., *Role of Kinetic Factors in Chemical Vapor Deposition Synthesis of Uniform Large Area Graphene Using Copper Catalyst.* Nano Letters, 2010. **10**(10): p. 4128-4133.
- 34. Li, X., et al., *Large-area graphene single crystals grown by low-pressure chemical vapor deposition of methane on copper*. J Am Chem Soc, 2011. **133**(9): p. 2816-9.
- 35. Chen, S., et al., Oxidation resistance of graphene-coated Cu and Cu/Ni alloy. ACS Nano, 2011. 5(2): p. 1321-7.
- 36. Cho, J., et al., *Atomic-scale investigation of graphene grown on Cu foil and the effects of thermal annealing*. ACS Nano, 2011. **5**(5): p. 3607-13.
- 37. Chen, H., W. Zhu, and Z. Zhang, Contrasting behavior of carbon nucleation in the initial stages of graphene epitaxial growth on stepped metal surfaces. Phys Rev Lett, 2010. **104**(18): p. 186101.
- 38. Jacobberger, R.M. and M.S. Arnold, *Graphene Growth Dynamics on Epitaxial Copper Thin Films*. Chemistry of Materials, 2013. **25**(6): p. 871-877.
- 39. Lopez, G.A. and E. Mittemeijer, *The solubility of C in solid Cu*. Scripta Materialia, 2004. **51**(1): p. 1-5.
- 40. Li, X.S., et al., Evolution of Graphene Growth on Ni and Cu by Carbon Isotope Labeling. Nano Letters, 2009. **9**(12): p. 4268-4272.
- 41. Yan, K., et al., Formation of Bilayer Bernal Graphene: Layer-by-Layer Epitaxy via Chemical Vapor Deposition. Nano Letters, 2011. 11(3): p. 1106-1110.
- 42. Robertson, A.W. and J.H. Warner, *Hexagonal Single Crystal Domains of Few-Layer Graphene on Copper Foils*. Nano Letters, 2011. **11**(3): p. 1182-1189.
- 43. Gao, L., J.R. Guest, and N.P. Guisinger, *Epitaxial Graphene on Cu(111)*. Nano Letters, 2010. **10**(9): p. 3512-3516.
- 44. Zhou, H.L., et al., *Chemical vapour deposition growth of large single crystals of monolayer and bilayer graphene.* Nature Communications, 2013. **4**.
- 45. Li, J., et al., *Impurity-induced formation of bilayered graphene on copper by chemical vapor deposition.* Nano Research, 2016. **9**(9): p. 2803-2810.
- 46. Luo, Z.T., et al., Effect of Substrate Roughness and Feedstock Concentration on Growth of Wafer-Scale Graphene at Atmospheric Pressure. Chemistry of Materials, 2011. 23(6): p. 1441-1447.
- 47. Zhang, B., et al., Low-Temperature Chemical Vapor Deposition Growth of Graphene from Toluene on Electropolished Copper Foils. Acs Nano, 2012. **6**(3): p. 2471-2476.
- 48. Miseikis, V., et al., *Rapid CVD growth of millimetre-sized single crystal graphene using a cold-wall reactor*. 2d Materials, 2015. **2**(1).
- 49. Withanage, S., et al., *The role of surface morphology on nucleation density limitation during the CVD growth of graphene and the factors influencing graphene wrinkle formation.* MRS Advances, 2019. **4**(61-62): p. 3337-3345.
- 50. Li, X.S., et al., *Graphene Films with Large Domain Size by a Two-Step Chemical Vapor Deposition Process.* Nano Letters, 2010. **10**(11): p. 4328-4334.
- 51. Miseikis, V., et al., *Deterministic patterned growth of high-mobility large-crystal graphene: a path towards wafer scale integration.* 2d Materials, 2017. **4**(2).
- 52. Gan, L. and Z.T. Luo, *Turning off Hydrogen To Realize Seeded Growth of Subcentimeter Single-Crystal Graphene Grains on Copper*. Acs Nano, 2013. 7(10): p. 9480-9488.
- 53. Xu, X.Z., et al., *Ultrafast growth of single-crystal graphene assisted by a continuous oxygen supply*. Nature Nanotechnology, 2016. **11**(11): p. 930-935.
- 54. Woehrl, N., et al., *Plasma-enhanced chemical vapor deposition of graphene on copper substrates*. Aip Advances, 2014. **4**(4).
- 55. Yeh, N.C., et al., Single-step growth of graphene and graphene-based nanostructures by plasma-enhanced chemical vapor deposition. Nanotechnology, 2019. **30**(16).
- 56. Li, M.L., et al., Controllable Synthesis of Graphene by Plasma-Enhanced Chemical Vapor Deposition and Its

- Related Applications. Advanced Science, 2016. 3(11).
- 57. Geng, D.C., et al., *Uniform hexagonal graphene flakes and films grown on liquid copper surface*. Proceedings of the National Academy of Sciences of the United States of America, 2012. **109**(21): p. 7992-7996.
- 58. Yuan, G., et al., Proton-assisted growth of ultra-flat graphene films. Nature, 2020. 577(7789): p. 204-208.
- 59. Zhang, Y., et al., Vapor Trapping Growth of Single-Crystalline Graphene Flowers: Synthesis, Morphology, and Electronic Properties. Nano Letters, 2012. 12(6): p. 2810-2816.
- 60. Meca, E., et al., Epitaxial Graphene Growth and Shape Dynamics on Copper: Phase-Field Modeling and Experiments. Nano Letters, 2013. 13(11): p. 5692-5697.
- 61. Yan, Z., et al., Toward the Synthesis of Wafer-Scale Single-Crystal Graphene on Copper Foils (vol 6, pg 9110, 2012). Acs Nano, 2013. **7**(3): p. 2872-2872.
- 62. Khaksaran, M.H. and I.I. Kaya, *On the Dynamics of Intrinsic Carbon in Copper during the Annealing Phase of Chemical Vapor Deposition Growth of Graphene*. Acs Omega, 2019. **4**(6): p. 9629-9635.
- 63. Kostogrud, I.A., K.V. Trusov, and D.V. Smovzh, *Influence of Gas Mixture and Temperature on AP-CVD Synthesis of Graphene on Copper Foil.* Advanced Materials Interfaces, 2016. **3**(8).
- 64. Wu, Y.P., et al., Effects of thermally-induced changes of Cu grains on domain structure and electrical performance of CVD-grown graphene. Nanoscale, 2016. **8**(2): p. 930-937.
- 65. Wu, B., et al., Self-organized graphene crystal patterns. Npg Asia Materials, 2013. 5.
- 66. Zhuang, J.N., et al., *Morphology Evolution of Graphene during Chemical Vapor Deposition Growth: A Phase-Field Theory Simulation*. Journal of Physical Chemistry C, 2019. **123**(15): p. 9902-9908.
- 67. Kobayashi, R., Modeling and Numerical Simulations of Dendritic Crystal-Growth. Physica D, 1993. **63**(3-4): p. 410-423.
- 68. Artyukhov, V.I., et al., *Breaking of Symmetry in Graphene Growth on Metal Substrates*. Physical Review Letters, 2015. **114**(11): p. 115502.
- 69. Fan, L., et al., *Topology evolution of graphene in chemical vapor deposition, a combined theoretical/experimental approach toward shape control of graphene domains.* Nanotechnology, 2012. **23**(11): p. 115605.
- 70. Hayashi, K., S. Sato, and N. Yokoyama, *Anisotropic graphene growth accompanied by step bunching on a dynamic copper surface*. Nanotechnology, 2013. **24**(2).
- 71. Wofford, J.M., et al., *Graphene Islands on Cu Foils: The Interplay between Shape, Orientation, and Defects.* Nano Letters, 2010. **10**(12): p. 4890-4896.
- 72. Tian, J.F., et al., Graphene Induced Surface Reconstruction of Cu. Nano Letters, 2012. 12(8): p. 3893-3899.
- 73. Paronyan, T.M., et al., Formation of Ripples in Graphene as a Result of Interfacial Instabilities. Acs Nano, 2011. 5(12): p. 9619-9627.
- 74. Yoon, D., Y.W. Son, and H. Cheong, *Negative Thermal Expansion Coefficient of Graphene Measured by Raman Spectroscopy.* Nano Letters, 2011. **11**(8): p. 3227-3231.
- 75. Deng, B., et al., *Anisotropic Strain Relaxation of Graphene by Corrugation on Copper Crystal Surfaces*. Small, 2018. **14**(22): p. 1800725.
- 76. Hao, Y.F., et al., *The Role of Surface Oxygen in the Growth of Large Single-Crystal Graphene on Copper.* Science, 2013. **342**(6159): p. 720-723.
- 77. Gottardi, S., et al., *Comparing Graphene Growth on Cu(111) versus Oxidized Cu(111)*. Nano Letters, 2015. **15**(2): p. 917-922.
- 78. Jia, C.C., et al., *Direct Optical Characterization of Graphene Growth and Domains on Growth Substrates*. Scientific Reports, 2012. **2**.
- 79. Vlassiouk, I., et al., *Graphene Nucleation Density on Copper: Fundamental Role of Background Pressure.* The Journal of Physical Chemistry C, 2013. **117**(37): p. 18919-18926.
- 80. Kang, J.H., et al., *Strain Relaxation of Graphene Layers by Cu Surface Roughening*. Nano Letters, 2016. **16**(10): p. 5993-5998.
- 81. Luo, B., et al., *Etching-Controlled Growth of Graphene by Chemical Vapor Deposition*. Chemistry of Materials, 2017. **29**(3): p. 1022-1027.
- 82. Vlassiouk, I., et al., *Role of Hydrogen in Chemical Vapor Deposition Growth of Large Single-Crystal Graphene*. ACS Nano, 2011. **5**(7): p. 6069-6076.
- 83. Li, Q., et al., *Hydrogen Induced Etching Features of Wrinkled Graphene Domains*. Nanomaterials (Basel), 2019. **9**(7).
- 84. Fan, L., et al., *Step driven competitive epitaxial and self-limited growth of graphene on copper surface.* AIP Advances, 2011. **1**(3): p. 032145.

Declaration of interests			

Interests or personal relationship
that could have appeared to influence the work reported in this paper.
☐The authors declare the following financial interests/personal relationships which may be considered
as potential competing interests: